Phase transitions in two planar lattice models and topological defects: A Monte Carlo study

Subhrajit Dutta and Soumen Kumar Roy
Department of Physics, Jadavpur University, Calcutta 700 032, India
(Received 19 February 2004; revised manuscript received 27 August 2004; published 17 December 2004)

Monte Carlo simulation has been performed in the planar P_2 and P_4 models to investigate the effects of the suppression of topological defects on the phase transition exhibited by these models. Suppression of the $1/2$ defects on the square plaquettes in the P_2 model leads to complete elimination of the phase transition observed in this model. However, in the P_4 model, on suppressing the single $1/2$ defects on square plaquettes, the otherwise first order phase transition changes to a second order one which occurs at a higher temperature, and this is due to the presence of a large number of $1/2$ pair defects which are left within the square plaquettes. When we suppressed these charges too, complete elimination of the phase transition was observed.

DOI: 10.1103/PhysRevE.70.066125 PACS number(s): 64.60.−i, 61.30.Jf

I. INTRODUCTION

It is well known that conventional long range order cannot exist in a two-dimensional continuous spin system [1]. However, the existence of topological charges leads to a quasi long range order (QLRO) to disorder phase transition. The most notable and thoroughly investigated example is the two-dimensional *XY* model [$O(2)$ model] in which, using a renormalization group technique, Kosterlitz and Thouless [2] predicted a QLRO-disorder phase transition which is associated with the unbinding of the vortex-antivortex pairs (topological charges of strength ± 1) which are stable topological defects in this system. The phase with QLRO is characterized by an algebraic decay of the spin-spin correlation function which is a slower decay than the fast exponential one which is observed in a completely disordered system. On the other hand, in the two-dimensional nonlinear sigma model, an example of which is the planar $O(3)$ model, there exists no stable topological defect and the system remains disordered at all finite temperature [3].

Another class of the two-dimensional systems of interest is the planar Lebwohl-Lasher (LL) [4] model and a modified version of it to be elaborated below. In the three-dimensional version of the LL model, the spins (of dimensionality 3), located at the sites of a simple cubic lattice, interact with nearest neighbors via a potential $-P_2(\cos\theta)$ where θ is the angle between the spins and P_2 is the second Legendre polynomial. This model successfully describes the orientational aspects of a nematic and undergoes a weakly first order phase transition, representative of the nematic-isotropic (NI) transition, seen in a real nematic. A number of investigators [5,6] have used a modified version of the LL model by adding a $-P_4$ term to the usual $-P_2$ one, P_4 being the fourth order Legendre polynomial. The introduction of the P_4 term reduces the sharpness of the peak of the P_2 term in the potential at $\theta=\pi/2$ and may lead to the appearance of a local minimum, depending on the relative strengths of the P_2 and P_4 terms in the potential. This is found to enhance the first order degree of the NI transition.

The two-dimensional version of the LL model and a modified version of it with a pure P_4 interaction between nearest neighbor spins have recently been investigated using Monte Carlo (MC) methods by a number of authors [7–9]. In the rest of this paper we shall refer to these as the planar P_2 and P_4 models, respectively. Both models possess in addition to the usual $O(3)$ symmetry, a Z_2 symmetry as well and this leads to the identification of the antipodal points in the order parameter space S^2. The planar P_2 model is known to exhibit a continuous phase transition at a dimensionless temperature whose thermodynamic limit is 0.547 [8] and the P_4 model is characterized by a strongly first order transition at temperature 0.376 [9]. In the low temperature ordered phase in both models the pair correlation function shows an algebraic decay to a plateau which changes over to an exponential decay in the neighborhood of the phase transition [8,9].

The role of defects in the phase transition of various three-dimensional spin systems is very difficult to study theoretically due to the nonlinearity introduced in the three-dimensional (3D) nature of the spins. However, a simulation technique may be used to investigate the role of topological defects in these systems. Lau and Dasgupta [10] have shown numerically using the conventional METROPOLIS algorithm that monopoles (hedgehogs) are necessary for the phase transition in the three-dimensional Heisenberg model. These authors observed that if one suppresses the formation of these defects in the 3D Heisenberg model, the system remains ordered at all temperatures and the transition to the disordered phase disappears altogether. The present work, which involves an elaborate MC study, was undertaken to investigate the effect of the suppression of the topological defects on the phase transitions which the planar P_2 and P_4 models exhibit. The work was motivated to a large extent by the work of Lau and Dasgupta [10] in the 3D Heisenberg model. Other work, along the same line, which must be mentioned in this context, is that of Lammert *et al.* [11] who, in a MC study, have shown that the nature of the nematic-isotropic transition in a 3D nematic changes when one suppresses the formation of the stable line defects, called the disclination lines. Our work shows that the topological defects play a very crucial role in the phase transition in the planar P_2 and P_4 models and although these models possess the same symmetry they have remarkably different critical behavior.

In the next section we briefly discuss the nature of the topological defects in the planar P_2 and P_4 models and the

algorithms for their identification are presented in the following one. The details of our MC simulation are then presented followed by the results and discussion.

II. Topological defects in the planar models

In the two-dimensional Heisenberg model there exist no stable topological defects. So the first or fundamental homotopy group is just the set containing the identity. However, in the present planar models (P_2 and P_4) due to the local Z_2 symmetry in addition to the $O(3)$ symmetry there arise stable topological point defects known as $1/2$ disclination points, where the director rotates through an angle of 180° around the defect core. The order parameter space is just the unit sphere S^2 with antipodal points identified. Any mapping of the other half integral point defects on the order parameter space is homotopically equivalent to the mapping of the $1/2$ defect. Point defects of integral strength are not stable in these models because of the so called escape to the third dimension. Any attempt to escape from a configuration containing a $1/2$ point defect leads to a more singular semi-infinite line defect extending from the defect core. So the fundamental or first homotopy group of the concerned models is just the two-element group Z_2 [12],

$$\pi_1 = \{0,1\}.$$

It is known that topological instability does not necessarily imply physical instability [12]. If the path connecting the singular to nonsingular configurations of the free energy involves a configuration of higher free energy than either, then one may say that the topologically unstable singularity may possess a considerable degree of physical metastability. This seems to happen in the P_4 model and may be briefly explained as follows. Consider a configuration where each of the four spins at the lattice sites which form a unit square are in a plane and oriented at right angle to their neighbors. The $-P_4(\cos\theta)$ potential, in addition to having the global minimum at $\theta=0$ (or $\theta=\pi$), also has a local minimum at $\theta=\pi/2$. If the orientation of the spins are now gradually changed in order to make $\theta\rightarrow 0$ (so as to reach the ground state) a potential barrier will have to be overcome and the process becomes energetically costly. Thus there may exist metastable integral point defects in this model [13].

The algorithm for the detection of these defects is, however, nontrivial as it is not really possible to enclose a 1 defect by four spins alone. The possible method of detection of these defects is discussed in the next section. We add that we were unable to detect any such defect because of the low probability of their formation.

III. The Defect finding algorithms

In order to detect the $1/2$ point defects we have followed the algorithm originally proposed by Vachaspati [14] and subsequently used by others [15]. In order to trace out the topological defects it will be useful to see when a closed loop in the physical space will enclose a $1/2$ disclination point. Let us consider a triangular plaquette *ABC* in the physical space. Due to local inversion symmetry we have to assign

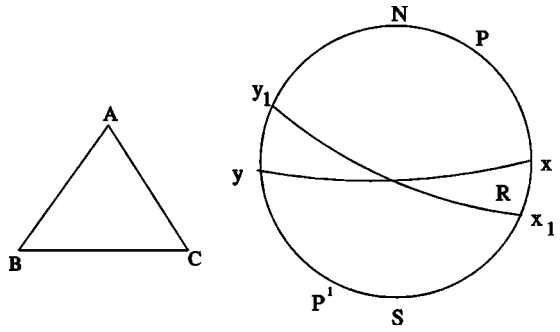

FIG. 1. The triangular plaquette *ABC* in physical space (left) and the order parameter space (right). On S^2 (N,S) is assigned for A, (P,P^1) for B, and (R,R^1) for C. The great circle xy is perpendicular to NS and x_1y_1 is perpendicular to PP^1. If the point R is outside the region enclosed by two great circles then the corresponding loop is contractible, otherwise *ABC* will enclose a $1/2$ disclination point (see Ref. [14]).

antipodal pair points on the unit sphere (S^2) for each site of the triangular plaquette. Let points corresponding to A, B, and C be (N,S), (P,P^1), and (R,R^1) (Fig. 1). Let us start from the north pole N. The point P or P^1 is selected depending on which is closer to N. Let P be the selected point. So the arc NP of the great circle on the order parameter space is traversed when we go from site A to B on the physical space. Select from R or R^1 whichever is closer to P. If the selected point is closer to S then the mapping of *ABC* is a noncontractible loop and the plaquette will enclose a $1/2$ disclination point defect. However, if the selected point for C is closer to N, then the mapping is contractible to a point on the sphere and no defect will be enclosed by the triangular plaquette. It may be noted that if S_i, S_j, and S_k are the spin variables associated with the points A, B, and C then the triangular plaquette will enclose a $1/2$ defect if

$$\mathrm{sgn}[(S_i,S_j)(S_j,S_k)(S_k,S_i)] = -1. \tag{1}$$

Priezev and Pelcovits [6] in their work on three-dimensional nematics have defined defect counting operators based on this principle. In addition to these two mathematically equivalent methods, an algorithm for detecting $1/2$ defects in RP^2 models can be developed using the method first proposed by Berg and Luscher [16]. The method works as follows. The projection matrix P associated with each unit spin vector S in an RP^2 model obeys the relation $P^2=P$ and $\mathrm{Tr}P=1$ and its elements may be defined as $P_{\alpha\beta}=S_\alpha S_\beta$ where $\alpha,\beta=1,2,3$. The charge at a lattice site x^* enclosed by an elementary triangular plaquette which has the projection matrices P_1, P_2, and P_3 associated with its corners is given by

$$q_{x^*} = \frac{1}{2\pi}\cos^{-1}\frac{\mathrm{Tr}\{P_3P_2P_1\}}{\{\mathrm{Tr}P_1P_2\mathrm{Tr}P_2P_3\mathrm{Tr}P_3P_1\}^{1/2}}. \tag{2}$$

We have used and checked that all the three above mentioned algorithms for the detection of the $1/2$ defects in triangular plaquettes are exactly equivalent in all cases in both models.

The detection of the metastable 1 defects in the P_4 model is a nontrivial job and the probability of their formation is

very low as this requires a very "special arrangement of the order parameter over many uncorrelated domains" [17]. In 3D nematics, where in principle both line and point defects (hedgehogs) may form, no point defects are observed in experiments on quenched nematics [18] until the defect network has coarsened appreciably. It has been observed that monopoles were formed only by string interactions and none were generated during the quench. Using the topology, on more specifically the homology, of the order parameter space [17], Hindmarsh has explained why the expected density of point defects is extremely low. The observation, briefly speaking, is that in order to cover RP^2 space twice (which is necessary for a topological 1 charge) a roughly spherical arrangement of a minimum of 12 uncorrelated adjacent domains is necessary and this has a probability $\sim 10^{-8}$. In a two-dimensional nematic the same considerations are believed to apply for the +1 point defects [19]. We have used the algorithm using the 12-spin configuration proposed by Zapotacky *et al.* [15] to detect the 1 charge but could find none.

IV. The Simulation Details

In the present paper we have used the conventional METROPOLIS spin update algorithm [20,21] with periodic boundary conditions in order to study the role of the topological defects in the phase transitions exhibited by the planar P_2 and P_4 models. Lattice sizes ranging from 20×20 to 80×80 were used and a part of the work was performed using the histogram reweighting technique of Ferrenberg and Swendsen [22].

In order to carry out the procedure of the suppression of the defects in the planar lattice models we have included a chemical potential term associated with the topological charges [10]. The Hamiltonian used in the simulation is given by

$$H = -\sum_{ij} P_L(\cos\,\theta_{ij}) + \lambda \sum_{ijkl} Q_{ijkl} \tag{3}$$

where L is either 2 or 4. θ_{ij} is the angle between the nearest neighbor spins i,j and Q_{ijkl} is the sum of charges of two triangular portions of a square plaquette. A positive λ makes the formation of the charges expensive in terms of energy and for almost total suppression of the charge a large value of λ (about 10 to 60, but independent of temperature) was normally chosen. In order to obtain an unrestricted simulation we set $\lambda = 0$. The charge enclosed by ijk for instance is given by

$$Q_{ijk} = \tfrac{1}{4}[1 - \mathrm{sgn}\{(S_i,S_j)(S_j,S_k)(S_k,S_i)\}]. \tag{4}$$

Clearly the sum Q_{ijkl} can be 0, 1/2, or 1. If Q_{ijkl} is 0 then the square plaquette encloses no charge. If it is 1/2 then a 1/2 disclination point is enclosed. But if it is 1, then it should not be confused with an integral point defect. In fact this corresponds to two closest possible 1/2 charges situated within a square plaquette of linear dimension equal to the lattice spacing.

In both the planar models we have investigated, the smallest part of the system in real space that can enclose a 1/2 point defect is a triangle. Each elementary square plaquette can be diagonally cut into two triangles and if these two adjacent triangles each enclose a 1/2 defect then this leads to a 1/2 pair charge being enclosed by the elementary square. If only one of those triangles encloses a 1/2 charge then the square in turn encloses a single 1/2 charge. We denote the number of square plaquettes enclosing a pair of 1/2 charges by n_1 (this should, however, not be confused with a topological defect of charge 1). Similarly, the number of elementary squares enclosing a single 1/2 charge is denoted by $n_{1/2}$. In a recent work, Mondal and Roy [13] have observed that the ratio $n_{1/2}/n_1$ behaves like a response function in both the models although its behavior is different in the two systems. When plotted against temperature, the ratio $n_{1/2}/n_1$ exhibits a maximum at the transition in the P_2 model while in the P_4 model it shows a sharp fall at the transition. Finite size effects are also prominent in the transition temperatures thus obtained from the $n_{1/2}/n_1$ vs T plots.

In our MC simulation, while investigating the effect of suppression for the charges in the two planar models, we have treated the single 1/2 charge and the 1/2 pairs (within an elementary square plaquette) on different footings. For the simulation where no charge suppression has been attempted we have set $\lambda = 0$. For the suppression of the charges represented by $n_{1/2}$, $\lambda \neq 0$ only for $Q_{ijkl} = 1/2$ while for total (both single-1/2 and 1/2-pair suppression), $\lambda \neq 0$ for $Q_{ijkl} \neq 0$. In the P_2 model, complete suppression of single 1/2 defects was found to lead to complete suppression of the 1/2 pair defects and this leads to complete elimination of the phase transition in this model. In the P_4 model, however, the suppression of the single 1/2 defects leaves a large number of 1/2 pair defects within the elementary squares and evidence of an additional phase transition at a higher temperature is obtained. When these defects too are suppressed, the phase transition totally disappears.

In order to estimate the critical exponents and the thermodynamic limit of the critical temperature of the transition that we obtained in the P_4 model and which seems to be of second order, we have applied the finite size scaling method. The finite size scaling method is a technique of estimating the critical exponents and the thermodynamic limit of the transition temperature by observing how the measured quantities vary with the system size. In the finite size scaling method (the data collapse method in particular) we extract the part of the thermodynamic function which does not contain the system size explicitly [21]. This part is called the scaling function. If proper values of the critical exponents and the thermodynamic limit for the transition temperature are chosen then the scaling function for different system sizes collapses. In this paper we have used the data collapse technique for estimating the critical exponents associated with the specific heat and the order parameter. The critical exponents associated with the correlation length, specific heat, and order parameter are denoted by ν, α, and β, respectively.

For the specific heat, the scaling relation stands as

$$C_V = L^{\alpha/\nu}\tilde{C}(L^{1/\nu}t) \tag{5}$$

where t is the reduced temperature and $\tilde{C}$ is the specific heat scaling function.

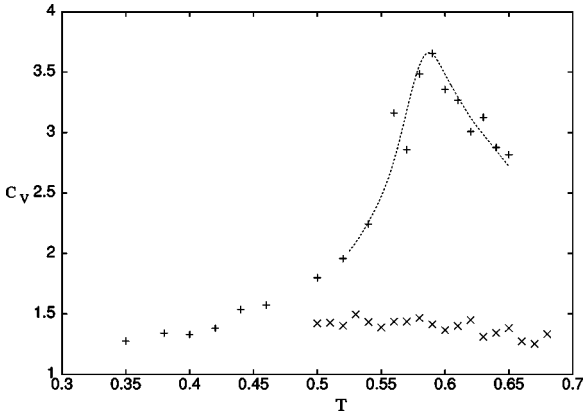

FIG. 2. The specific heat vs temperature plot in the P_2 model. + corresponds to C_V obtained from energy fluctuation in the $L=40$ lattice and the continuous curve is taken from Ref. [8] where it has been obtained using multiple histogram reweighting and the peak is at $T=0.587$. Both correspond to normal MC simulation with no charge suppression. The $\times$ represents C_V for $L=40$ lattice after suppressing the single $1/2$ defects on the square plaquettes.

Similarly for the order parameter $\langle q^2 \rangle$ [see Eq. (7)], the scaling relation is given by

$$\langle q^2 \rangle = L^{-4\beta/\nu} \tilde{Q}(L^{1/\nu} t) \tag{6}$$

where $\tilde{Q}$ is known as the order parameter scaling function [11].

V. RESULTS AND DISCUSSION

We have evaluated various thermodynamic properties like the internal energy per particle $\langle E \rangle$, specific heat, order parameter, etc. The specific heat was evaluated by taking the temperature derivative of $\langle E \rangle$ as well as from fluctuation of the energy. Due to the local inversion symmetry, the order parameter is a second rank tensor.

As a measure of the order prevailing in the system we used the quantity $\langle q^2 \rangle$ given in Ref. [11]:

$$\langle q^2 \rangle = \frac{N}{N-1} \left\langle \frac{3}{2} \mathrm{Tr} Q^2 - \frac{1}{N} \right\rangle \tag{7}$$

where $Q_{ab} = (1/N) \Sigma Q(i)_{ab}$ is the nematic tensor order parameter, $Q(i)_{ab} = \left(n_a n_b - \frac{1}{3}\delta_{ab}\right)$ ($\hat{n}$ is the molecular axis of the ith molecule), and N is the total number of sites (i) in the lattice. This definition ensures that $\langle q^2 \rangle$ is zero in a fully disordered system and 1 for a fully ordered system.

In the case of the P_2 model we have simulated for linear dimension $L=40$ and 60. In Fig. 2 we have depicted the specific heat versus temperature plot for the P_2 lattice model of size 40×40. The unrestricted simulation shows a peak that disappears when the single $1/2$ charges on the square plaquettes are suppressed. We have observed that the after suppression of the single $1/2$ charges on the square plaquettes there remains no $1/2$ pair defect in any square plaquette. The temperature dependence of the order parameter used in this model for the two cases is shown in Fig 3.

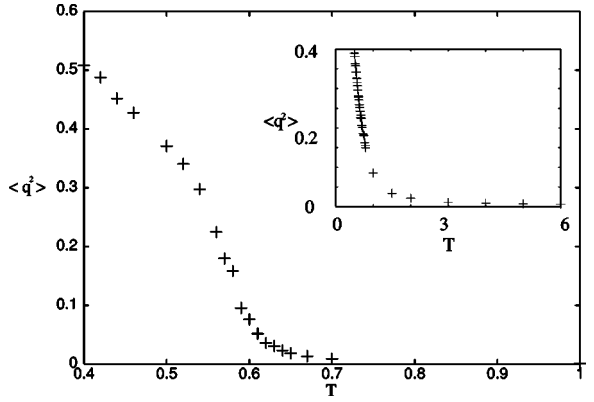

FIG. 3. The order parameter $\langle q^2 \rangle$ obtained for the $L=40$ lattice in the P_2 model with no charge suppression. The temperature derivative has a peak at $T=0.567$. The inset shows the $\langle q^2 \rangle$ vs T plot after suppressing the single $1/2$ defects on the square plaquettes.

While the temperature derivative of $\langle q^2 \rangle$ has a peak at the transition temperature in the normal case (where no defect is suppressed), which presumably is a signal of a phase transition in a finite system [23], in the defect-free case it seems to lose the characteristic shape and shows a smooth and rather slow decrease with temperature and vanishes at around a temperature $T=6$. We would be inclined to conclude from the results on C_V and $\langle q^2 \rangle$ that the defect-free phase exhibits no phase transition at all.

Turning to the P_4 model, which has a characteristic strongly first order phase transition [9], we first point out that the suppression of the single $1/2$ defects on the square plaquettes here does not result in suppression of the $1/2$ pair defects on the square plaquettes. This observation is different from what happens in the P_2 system where the suppression of the single $1/2$ defects on the square plaquettes leads to suppression of the $1/2$ pair defects. On suppressing the single $1/2$ defects a different phase transition is observed. We point out, however, that it is impossible to make the system completely free of topological defects, even when arbitrarily large values of λ are used. However, the residual charges left were of very insignificant amount. For instance, at $T=0.55$, the traces of the single $1/2$ and $1/2$ pair charges that could not be suppressed were about 0.02% of these charges present in the system at the same temperature after single $1/2$ charge suppression. Figure 4 shows the temperature dependence of the specific heat for the normal lattice ($L=40$) and after suppression of the single $1/2$ defects (for $L=40$ and 60). The peak in C_V for the latter case, while is greatly reduced in size (from 80 to about 17), shifts to a higher temperature which for both lattices is close to 0.494. Presumably the phase transition that we observed after suppressing the single $1/2$ defects is due to the presence of the $1/2$ pair defects. When we suppressed the $1/2$ pair defects too in all triangular plaquettes of the lattice no evidence of any peak in C_V was observed, although a humplike feature was seen with $C_V \sim 3.5$ over a temperature range extending from 0.53 to 0.62. In the case of the P_4 model we have also investigated the response of the defect density to the phase transition. When no kind of charge suppression was applied a large number of single $1/2$ defects as well as $1/2$ pair de-

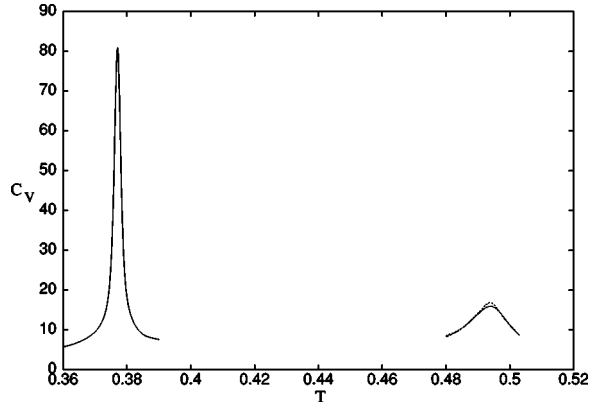

FIG. 4. C_V plotted against T for unrestricted simulation of $L=40$, P_4 lattice (left) and the same for $L=40$ and 60 lattices obtained after suppressing the single $1/2$ defects on the square plaquettes (right). The slightly bigger peak is for the $L=60$ lattice. The peak occurs at $T=0.494$.

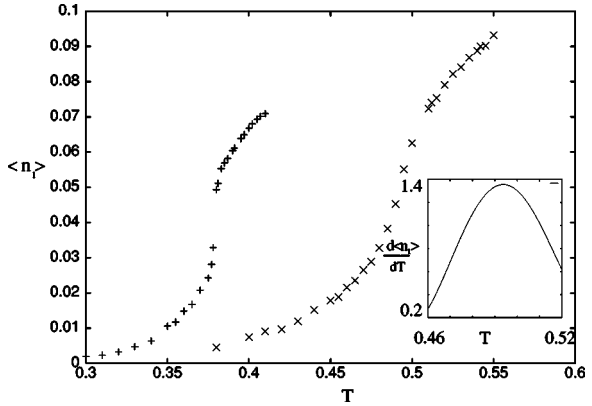

FIG. 6. The density $\langle n_1 \rangle$ of $1/2$ pair charges for the unrestricted case of the $L=40$ P_4 model (left) and the same after suppressing the single $1/2$ defects (right). The temperature derivative of the former has a peak at $T=0.379$ and the latter (inset) peaks at $T=0.494$.

fects were found to be present. In Fig. 5 the temperature dependence of the density of single $1/2$ defects is shown for unrestricted simulation. In Fig. 6 the temperature dependence of the density $1/2$ pair defects is shown both before and after suppression of the single $1/2$ defects. Clearly the temperature derivative of the defect density behaves like other response functions for all cases.

In Fig. 7, we have depicted the temperature dependence of the order parameter $\langle q^2 \rangle$ for all three cases in the P_4 model for $L=40$. The peaks of the temperature derivative of $\langle q^2 \rangle$ occur, respectively, at 0.379 (normal MC simulation) and 0.490 (after suppressing single $1/2$ defects) and their heights are 119.5 and 18.5, respectively. On suppressing all the $1/2$ charges on all triangular plaquettes of the lattice (total charge suppression), $d\langle q^2 \rangle / dT$ no longer exhibits a peak and $\langle q^2 \rangle$ seems to have an asymptotic value of 0.1 at $T=2$, up to which the investigation has been made. We add that $d\langle q^2 \rangle / dT$ after total charge suppression has a feature similar to that seen in C_V in that a broad peak of height ~ 4 was seen over a temperature range from 0.52 to 0.6. The existence of this broad hump of insignificant magnitude over an extended temperature range cannot be a sign of a phase transition. These, in some way, may be connected to the existence of the small number of residual charges left in the system after the attempt to suppress them completely failed.

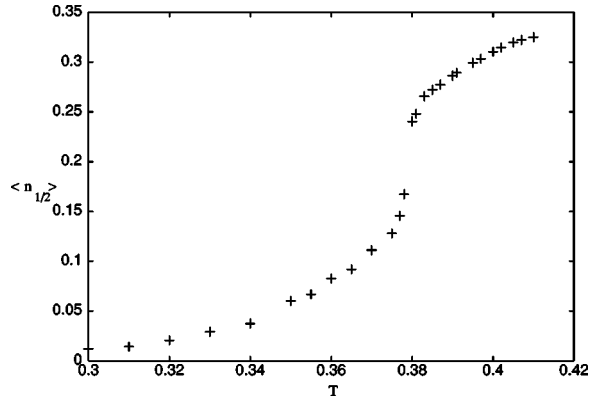

FIG. 5. The density of the single $1/2$ defects enclosed by the square plaquettes in the case of the $L=40$ P_4 model with no charge suppression.

We now turn to the pair correlation function $g(r) = \langle \cos^2 \theta_{ij} - 1/3 \rangle$ where r is the separation between the two spins i and j which make an angle θ_{ij} with each other. This function for the P_2 model at $T=0.6$, for instance, which is a temperature much higher than the normal critical temperature in this model, decays exponentially to zero, as it should, in the complete absence of long range order, and a best fit with $g(r) = \alpha \exp(-\lambda r)$ yields $\alpha = 0.439$ and $\lambda = 0.248$. For the single $1/2$ charge (and consequently $1/2$ pair charges) suppressed case, it decays algebraically and a best fit like $g(r) = ar^{-p} + b$ yields the parameters $a=0.404$, $b=0.022$, and $p=0.372$ (Fig. 8). In Fig. 9, the $g(r)$ vs r plots for the P_4 model are shown for $T=0.48$ (which is greater than the normal transition temperature but less than the transition temperature obtained after $1/2$-charge suppression), $T=0.5$ (which is

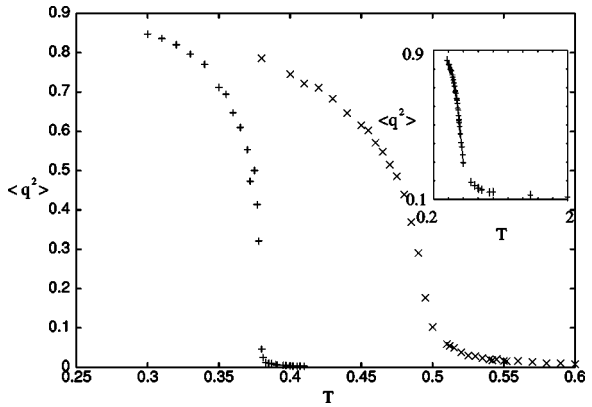

FIG. 7. The temperature dependence of $\langle q^2 \rangle$ for the $L=40$ P_4 model. On the left is the unrestricted MC result and on the right is the case when the single $1/2$ charges on the square plaquette were suppressed. The inset shows $\langle q^2 \rangle$ when all charges are suppressed. The temperature derivatives of the first two curves have peaks at 0.379 and 0.490, respectively.

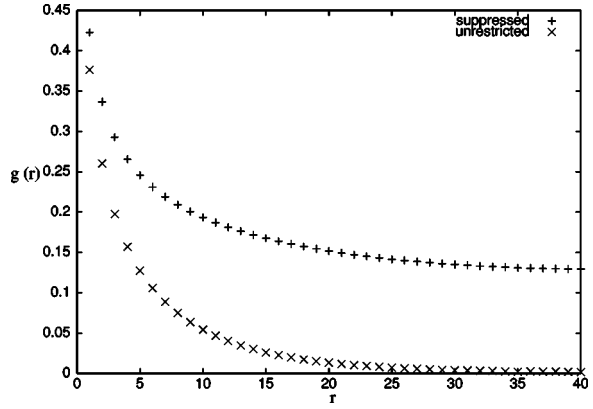

FIG. 8. The correlation function $g(r)$ plotted against r for the $L=40$ P_2 lattice at $T=0.6$ for both the unrestricted case and the suppressed case.

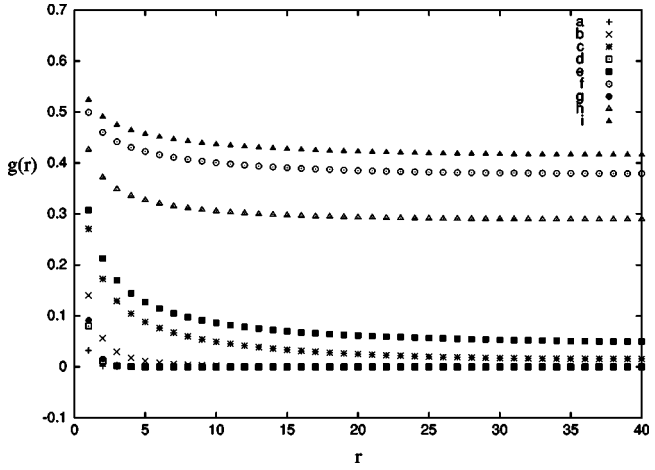

FIG. 9. The correlation function $g(r)$ plotted against r for the $L=80$ P_4 lattice. For the curves a, b, c, $T=0.68$; for the curves d, e, f, $T=0.5$, and for the curves g, h, i, $T=0.48$. The three curves in each set correspond to the normal MC, 1/2 charge suppressed, and total charge suppressed cases. The parameters used to fit these curves are listed in Table I.

slightly higher than the observed transition temperature after 1/2-charge suppression), and $T=0.68$. At all of these temperatures, as one would expect, the correlation function in the normal case decays exponentially to zero. The two other cases give best fits for an algebraic decay to a plateau, and the parameters are listed in Table I. We find that in the P_4 model the result of single-1/2-charge suppression is the same as that in the P_2 model, while with the suppression of the 1/2 pair charges too, the asymptotic value of the order prevailing in the system increases further. The phase transition that the P_4 system has after suppressing the single 1/2 charges is second order. We have evidence that it is not first order as the dual peak structure of the probability distribution as a function of energy, which is so distinct in the P_4 model [9], has been found to disappear totally after suppressing the single 1/2 charges on the square plaquettes. In Fig. 10 we have given the the free energy of 40×40 and 60×60 lattice in the P_4 model after suppressing the single 1/2 defects on the square plaquettes. The single well structure of the free energy indicates the second order quality of the phase transition after suppressing the single 1/2 defects.

We have also used standard finite size scaling method available for the second order phase transition [21] in order to estimate the critical exponents and the thermodynamic limit of the transition temperature of the phase transition that was observed after suppressing the single 1/2 defects. In Figs. 11 and 12 we have depicted the order parameter $\langle q^2\rangle$ and specific heat C_V plots, respectively, as functions of temperature for different lattice sizes after the single-1/2-charge suppression in the P_4 model. We have used the standard data collapse technique to collapse the data of Figs. 11 and 12 and the resulting diagrams are Figs. 13 and 14, respectively. In Fig. 13 we have shown the collapse of the order parameter scaling function for $L=20$, 40, 60, and 80, while in Fig. 14 the collapse of the specific heat scaling function for the system sizes 40, 60, and 80 are displayed. The data collapse clearly shows that the phase transition that the P_4 model exhibits after the single-1/2-charge suppression is second order. The parameters we have obtained are $T_c=0.498$, $\beta=0.16$, and $\nu=0.99$ for the collapse of the order parameter and $T_c=0.4938$, $\alpha=0.077$, and $\nu=0.94$ from the collapse of the specific heat. We would remark that the high-temperature behavior of the order parameter $\langle q^2\rangle$ after total charge suppression does not indicate the presence of a phase transition. This is true for both models.

We have used large values of λ in our simulation in order to suppress the evolution of defects in both models. It is known that any Monte Carlo study is faithful only if we can reach any point in the phase space starting from any other point. So there must be a path connecting the two points in phase space with nonzero probability. This actually indicates

TABLE I. The parameters obtained in the $L=80$, P_4 model for the best fit $g(r)=ar^{-p}+b$ of the correlation function at the temperatures indicated. In the normal lattice at these temperatures $g(r)$ decays exponentially to zero.

T	Charges suppressed	p	b
0.48	Single 1/2 suppressed on square plaquettes	0. 688	0. 275
0.48	Total	0. 432	0. 385
0.50	Single 1/2 suppressed on square plaquettes	0. 615	0. 062
0.50	Total	0. 474	0. 353
0.68	Single 1/2 suppressed on square plaquettes	1. 410	0
0.68	Total	0. 650	0

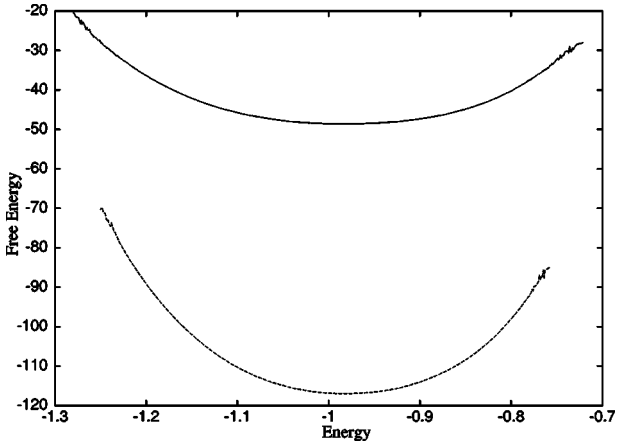

FIG. 10. Free energy vs energy for P_4 model for $L=40$ (upper) and $L=60$ (lower) sizes after suppressing the single $1/2$ defects on the square plaquettes.

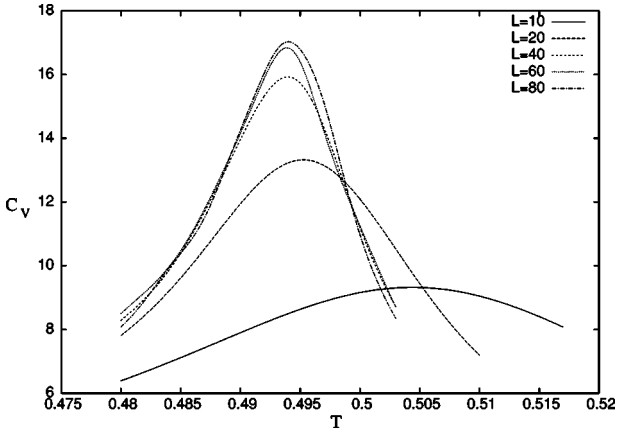

FIG. 12. The specific heat C_V vs T for the lattice sizes indicated for the P_4 model after the single $1/2$ charge suppression. The values of C_V here obtained from $d\langle E\rangle/dT$ and the histogram reweighting technique [22] was used.

that we should be careful that we are not trapped in any small region of the phase space. We have investigated the phase space connectivity in both the models by observing the evolution of the order parameter or energy with MC steps. The connectedness is satisfied if the observed quantities for different initial states converge to the same final value. In Fig. 15 we have shown that in case of the 80×80 P_2 model, after suppressing the $1/2$ defects (by using $\lambda=60$) on the square plaquettes, the final values of the order parameter is same for three different initial configurations. Similarly in Fig. 16 we have shown that the same thing happens for the total energy of the 80×80 P_4 model after suppressing the $1/2$ defects on the square plaquettes. It is therefore clear that we can use a value of λ at least up to 60 without violating the phase space connectivity.

VI. CONCLUSION

It is established in this paper that topological defects play a very important role in the phase transitions exhibited by the two planar lattice models we discussed. The observed difference in the critical behavior seems to be due to the difference in the role played by the topological defects. It is shown in this paper that for the phase transition in both models topological defects are necessary. In the P_2 model the phase transition is governed by the $1/2$ disclination points enclosed by the square plaquettes only (single $1/2$). On suppressing these single $1/2$ defects we have shown that the phase transition was totally eliminated. However, the picture is different in the case of the two-dimensional P_4 model, where on suppressing the single $1/2$ defects the nature and the transition temperature of the phase transition are changed. We have also shown that the phase transition in the P_4 model is due to the presence of a large number of $1/2$ pairs (enclosed by two triangular portions) within the square plaquettes which remains unsuppressed even after suppressing the single $1/2$ defects. This leads to another important conclusion that, for tracing out all the disclination points in two dimensions, the minimum closed loops in physical space to be considered are the smallest triangular cells formed by three nearest neighbor sites.

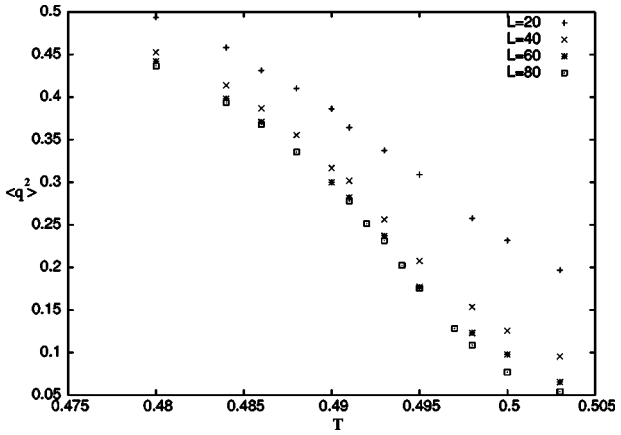

FIG. 11. The order parameter $\langle q^2\rangle$ plotted against temperature T for three lattice sizes indicated for the P_4 model after suppressing single $1/2$ defects.

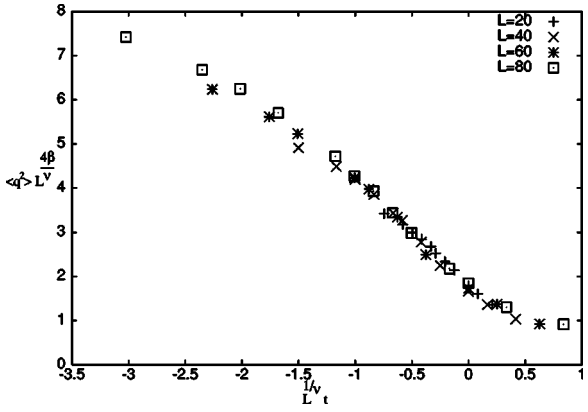

FIG. 13. Collapse of the order parameter for $L=20$, 40, 60, and 80 sizes. The best collapse is obtained at $T_c(\infty)=0.498$ (thermodynamic limit), $\nu=0.99$ (exponent for correlation length), $\beta=0.16$ (exponent for order parameter). t is the reduced temperature $(T-T_c)/T_c$.

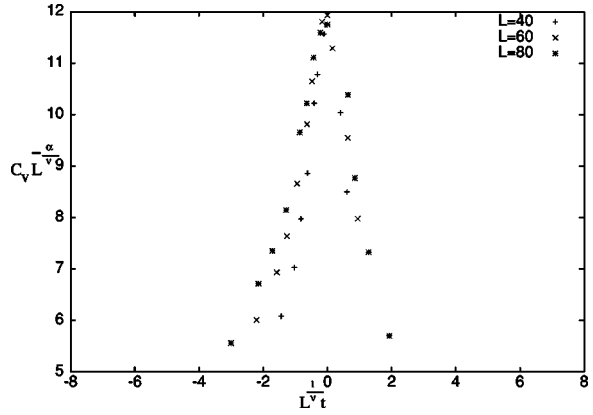

FIG. 14. The collapse of the specific heat data for system sizes $L=40$, 60, and 80. The best collapse obtained at the thermodynamic limit of the transition temperature $[T_c(\infty)=0.4938]$, $\nu=0.94$, and α (exponent for the specific heat) $=0.077$.

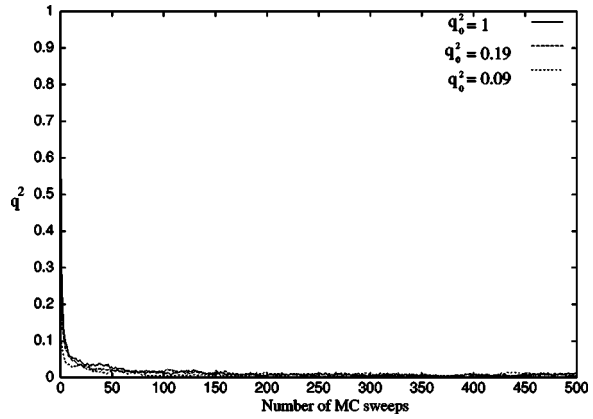

FIG. 15. Evolution of order parameter for 80×80 P_2 model after suppressing the $1/2$ defects enclosed by the square plaquettes using $\lambda=60$. The final values of the order parameter for three initial states with $q_0^2=1.0$, 0.19, and 0.09 are almost the same.

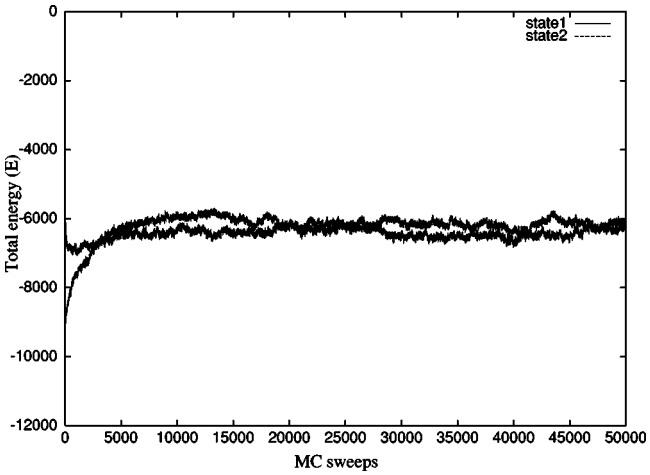

FIG. 16. Evolution of total energy of the 80×80 P_4 model after suppressing the $1/2$ defects enclosed by the square plaquettes using $\lambda=60$. The final values of energy for two different initial states are almost the same.

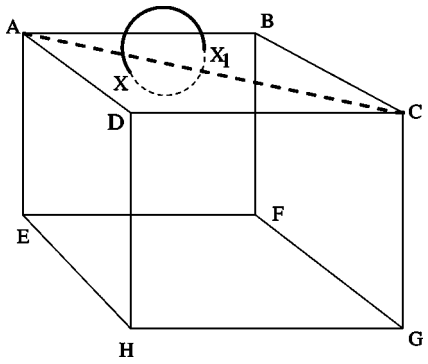

FIG. 17. The cubic unit cell *ABCDEFGH* in a three-dimensional nematic. The disclination ring cuts the upper face *ABCD* at X and X_1. The triangular portions *ABC* and *ADC* must enclose a $1/2$ defect each.

It will be interesting to apply the idea of triangular plaquettes in three-dimensional nematics, where the stable topological defects are disclination lines as well as monopoles. Let us consider a small disclination loop in a three-dimensional nematic (Fig. 17). In the figure a cubic unit cell *ABCDEFGH* is shown. The disclination loop has crossed the face *ABCD* twice. However, if we take mapping of *ABCD* on the order parameter space then we would get a contractible loop in the order parameter space and conclude that *ABCD* does not enclose any line defect. It is true that *ABCD* does not enclose a single line, but it encloses two close lines (as the loop intersects the face *ABCD* twice), which could be detected only if we consider the two triangular portions (*ABC* and *ADC*) of *ABCD*. So considering the elementary plaquettes to be square plaquettes of linear dimension equal to the lattice spacing, we would miss loops as shown in the figure. In real nematics small loops are known to carry monopole (hedgehog) charges. An actual monopole structure is very rare in real nematics. As already stated, the low probability of the actual monopole structure is discussed by Hindmarsh [17]. The monopoles that come into play in the three-dimensional nematics arise mainly from the small disclination rings. In our work it is evident that in the P_4 model it is very important to consider these triangular plaquettes in order to trace out the topological defects properly. If the same work is carried out on the three-dimensional P_4 model and disclination lines are traced out using triangular plaquettes, then one is likely to get a large number of rings as shown in Fig. 17. The small disclination rings which behave like monopoles, is expected to have an important role in the phase transition of the three dimensional P_4 model.

ACKNOWLEDGMENTS

The authors acknowledge a UGC Grant No. F.10-17/2001(SR-1) which enabled us to upgrade the computing facility. One of us (S.D.) acknowledges financial support from the Council of Scientific and Industrial Research (CSIR), India.

[1] N. D. Mermin and H. Wagner, Phys. Rev. Lett. **17**, 1133 (1966).
[2] J. M. Kosterlitz and D. J. Thouless, J. Phys. C **5**, L124 (1972); **5**, 1180 (1973).
[3] A. A. Migdal, Zh. Eksp. Teor. Fiz. **69**, 810 (1975); A. M. Polykov, Phys. Lett. **59B**, 79 (1975).
[4] P. A. Lebwohl and G. Lasher, Phys. Rev. A **6**, 426 (1972); **7**, 2222 (1973).
[5] Z. Zhang, O. G. Mouritsen, and M. J. Zuckermann, Phys. Rev. Lett. **69**, 2803 (1992); Z. Zhang, M. J. Zuckermann, and O. G. Mouritsen, Mol. Phys. **80**, 1195 (1993).
[6] N. V. Priezjev and R. A. Pelcovits, Phys. Rev. E **64**, 031710 (2001).
[7] H. Kunz and G. Zumbach, Phys. Rev. B **46**, 662 (1992).
[8] E. Mondal and S. K. Roy, Phys. Lett. A **312**, 397 (2003).
[9] A. Pal and S. K. Roy, Phys. Rev. E **67**, 011705 (2003).
[10] M. Lau and C. Dasgupta, Phys. Rev. B **39**, 7212 (1989).
[11] P. E. Lammert, D. S. Rokhsar, and J. Toner, Phys. Rev. E **52**, 1778 (1995); Phys. Rev. Lett. **70**, 1650 (1993).
[12] N. D. Mermin, Rev. Mod. Phys. **51**, 591 (1979).
[13] E. Mondal and S. K. Roy, Phys. Lett. A **324**, 337 (2004). (It may be noted that the mention of a topological 1 charge included in the elementary square plaquettes in this Letter should be replaced by 1/2 pair charges enclosed by the two elementary triangular plaquettes that form an elementary square).
[14] T. Vachaspati, Phys. Rev. D **44**, 3723 (1991).
[15] M. Zapotocky, P. M. Goldbart, and Nigel Goldenfeld, Phys. Rev. E **51**, 1216 (1995) (at the end of Sec. IV B the algorithm for finding the 360° defects is given).
[16] B. Berg and M. Luscher, Nucl. Phys. B **190**, 412 (1981).
[17] M. Hindmarsh, Phys. Rev. Lett. **75**, 2502 (1995).
[18] I. Chuang, R. Durrer, N. Turok, and B. Yurke, Science **251**, 1336 (1991); I. Chuang, B. Yurke, A. N. Pargellis, and N. Turok, Phys. Rev. E **47**, 3343 (1993).
[19] M. Hindmarsh (Ref. [17]), Ref. [15] therein.
[20] N. Metropolis *et al.*, J. Chem. Phys. **21**, 1087 (1953).
[21] M. E. J. Newman and G. T. Barkema, *Monte Carlo Methods in Statistical Physics* (Clarendon, Oxford, 1999).
[22] A. M. Ferrenberg and R. H. Swendsen, Phys. Rev. Lett. **63**, 1195 (1989).
[23] C. Chiccoli, P. Pasini, and C. Zannoni, Physica A **148**, 298 (1988); Liq. Cryst. **2**, 39 (1987).